sustainability

MDPI

Article

Numerical and Experimental Study on Propagation Attenuation of Leakage Vibration Acceleration Signal of the Buried Water Pipe

Xuan Yang [1,2], Fuming Wang [1,2], Xiang Yu [1,2,*] and Shaohui Li [1,2]

1 Yellow River Laboratory, Zhengzhou University, Zhengzhou 450001, China
2 School of Water Conservancy and Civil Engineering, Zhengzhou University, Zhengzhou 450001, China
* Correspondence: xiangyu@zzu.edu.cn

Abstract: For detecting water pipeline leakage signals, in the past people preferred to use sensors to obtain the leakage signal and then use various means and methods to remove noise to increase the positioning accuracy. However, as the leakage signal is generated, it spreads along the pipeline wrapped in soil. In this process, the signal will change significantly, eventually becoming very different from the original signal. As such, the detection accuracy will decline, as the detection distance becomes longer. Despite this, few researchers have considered the distortion caused by signal propagation in the whole process and instead use the distorted signal characteristics for positioning. This direction needs to be further studied. In this paper, the acceleration signal of leakage vibration is taken as the research object using a combination of tests and numerical simulation. The acceleration signals from the leakage source are collected and simulated at different distances. The reliability of the numerical simulation model is verified by using the inversion theory, and the influence of soil with different elastic modulus on the acceleration signal is expanded. Research findings: (a) For the attenuation of the acceleration signal of pipeline leakage vibration along the pipeline, the elastic modulus of soil around the pipeline in the numerical simulation model is about 3.3 times its compression modulus, which is closer to the actual situation. (b) The attenuation of the acceleration signal amplitude of pipeline leakage vibration conforms to the characteristics of an exponential function. The higher the elastic modulus of soil, the stronger the signal attenuation. (c) The soil with different elastic modulus has different absorption capacities to signal components, and the high-frequency part of the acceleration signal attenuates faster. (d) The group velocity of the leakage vibration signal is 929 m/s, and the different elastic modulus of soil will affect the group velocity of the leakage vibration signal.

Keywords: leak detection; signal attenuation law; elastic modulus of soil mass; group velocity

Citation: Yang, X.; Wang, F.; Yu, X.; Li, S. Numerical and Experimental Study on Propagation Attenuation of Leakage Vibration Acceleration Signal of the Buried Water Pipe. *Sustainability* **2022**, *14*, 16071. https://doi.org/10.3390/su142316071

Academic Editor: Md Mizanur Rahman

Received: 1 November 2022
Accepted: 26 November 2022
Published: 1 December 2022

1. Introduction

According to the *World Population Prospects 2022 Summary of Results* [1] report by the United Nations in July 2022, the global population could grow to around 8.5 billion in 2030, 9.7 billion in 2050, and 10.4 billion in 2100. With the growth of the world population, human demand for drinking water is increasing. However, the leakage rate of urban water supply pipelines remains high due to aging pipelines, limited investment in technical means, a backward regulatory system, and many other reasons [2]. However, the developing countries, which contributed significantly to the growth of the world population, have far higher leakage rates of urban water supply pipelines than the world average [3] because of their relatively backward economic and technological means. The leakage of water supply pipelines will not only cause the waste of water resources [4] and pollution [5], but also lead to accidents [6–8] such as road collapse and building collapse, resulting in a large number of casualties and property losses. Reducing the leakage rate has become an essential issue in the study of water supply pipelines. The first problem in reducing the leakage rate is locating the leakage. At present, the primary methods for this problem are artificial auditory recognition [9], ground penetrating radar [10], pipe robot [11], negative pressure wave [12], distributed optical fiber sensor detection [13,14], and other methods. The auditory recognition method relies too much on the experience of workers; however, the training of skilled workers requires high costs and the detection efficiency is low. The cost of the ground penetrating radar method is high, and it is exposed to misinformation about the buried metal body [15]. The robot method stops water detection, which quickly affects residents' daily lives. Since the water supply pipeline needs to open and close the water valve for water supply regulation from time to time, the negative pressure wave will often cause a false alarm.

The leak detection method of correlation analysis [16] has the characteristics of high detection efficiency, low detection cost, and does not stop water from affecting the lives of residents. It is a leak detection method that is used worldwide and can accurately locate the leak. The energy released by the pipe from elastic waves when it leaks is called acoustic emission [17]. The technique of leak detection by correlation analysis is to first place sensors on the pipe walls at both ends of the leak point. Then, respectively collect the vibration signals propagating along the pipe to both ends, and calculate the final position of the leak point using the time difference between the signals collected by the two sensors. Correlation analysis judges whether there is leakage by comparing the similarity of the signals received by two sensors. Nevertheless, the leakage port cannot always be located between two sensors. When the distance difference between the two sensors and the leakage port is large, the leakage signal may be distorted due to attenuation, frequency dispersion, and other reasons during the propagation process [18]. The signals received by the two sensors are so different that they cannot be accurately located. Therefore, it is of great practical and theoretical significance to study the propagation characteristics and mechanism of the leakage signal along the pipeline. In the past, many researchers have made many contributions in this direction. Hunaidi and Chu [19] conducted a systematic study on the acoustic signal and attenuation characteristics of water supply pipeline leakage as early as 1999 and made specific achievements. However, due to the environment and technology at that time, the research object was plastic pipes rather than the ductile iron ones used more commonly nowadays. The study's signal research scope was only within 200 Hz. Even the frequency domain of the transfer function is only 5–40 Hz. Updating the data with today's new technologies and equipment is urgent due to the current situation. R. Long et al. [20] further explained the relationship between the soil around the pipe and the acoustic signal propagation characteristics in 2002 based on the test. However, this study assumed that the leakage noise propagated in a non-dispersive manner, which is different from the actual situation and may lead to positioning errors. With further development of the relevant research, the research contents of various scholars are gradually deepened and more detailed. Yang et al. [21] put forward a new leak location method in 2008. This research uses a blind system identification strategy to estimate the transmission performance of two acoustic channels. It is not necessary to accurately obtain the pipeline length between two sensors during leak detection, which is helpful for the relevant research. Y. Gao et al. [22] focused on how wave reflection affects the cross-correlation function of two leakage noise signals used to detect and locate the leakage of buried water pipes. The reflection was introduced into the cross-correlation model to increase the positioning accuracy. However, the above two studies focus more on solving the algorithm problem of cross-correlation technology and rarely involve the more critical signal propagation rules and mechanisms. Su et al. [23] used acoustic transmitters and hydrophones to receive signals and constructed a method based on the propagation analysis of acoustic signals in tubes, achieving some results. However, in practical application, this method must stop water and place sensors, which fails to give full play to the advantages of cross-correlation technology. Jing et al. [24] simultaneously considered the characteristics of certainty and randomness and compared an inflatable acrylic pipe with a water-filled steel pipe. Furthermore, they proposed a modal-based analysis model to predict the propagation of sound waves in rigid and elastic pipes, which indicated that the water-filled steel pipe could be regarded as an elastic pipe.

However, this study only considered the pipe water coupling and did not consider the pipe soil coupling when the actual signal propagated. Abdullahi and Oyadiji [25] used finite element analysis to simulate the leakage of acoustic waves in liquid-filled pipes and used experimental means to verify it. However, the signal used in the finite element study is only a simple analog signal, not the vibration signal actually sampled, which cannot fully demonstrate the propagation of true signals. Yan et al. [26] measured the frequency spectrum characteristics of the leakage noise in a cast iron pipe and the nearby soil, using a triaxial seismic detector. However, in this test, the pipeline was not entirely buried in the soil, and so it could not fully reflect the influence of the soil on the leakage signal. Li et al. [27] deduced the three-dimensional transient leakage acoustic wave propagation equation by combining the fluid mechanics principles and Lighthill's acoustic analogy theory. Moreover, the propagation of leakage noise in the water supply pipeline was modeled theoretically. However, the model mainly described the propagation of the sound inside the pipe and did not involve the actual, more common external detection. Wu et al. [28] used the numerical analysis method to add a transmitter into the middle of the pipeline to simulate the leakage event and used the XGBoost algorithm to identify the leakage area and predict the leakage location. However, this study was only a numerical analysis, not an experimental verification, and its reliability needs further confirmation.

To sum up, the research mentioned above can provide significant help for the cross-correlation analysis method to identify the leakage location of a water supply pipeline. However, in general, there are still the following problems: (1) Most research only studies the pipeline leakage signal transmission through tests, but the test itself cannot exhaust various working conditions, so the laws cannot be better summarized. However, numerical simulation can fully simulate many working conditions with less cost, so the combination of tests and numerical research should be the focus of future research. (2) In some studies, the leakage signal of the numerical analysis part does not use the actual leakage signal, but only the analog signal. The analog signal cannot cover all the actual signal's characteristics, and its method's effectiveness for replacing the pipeline leakage signal must be further considered. (3) In the above research, more consideration is given either to the influence of the pipeline itself or the coupling between the pipeline and the water body on signal transmission. However, the actual pipeline is buried in the soil, so the influence of the soil should not be ignored. The soil around the buried pipeline is generally directly taken from the site, both in actual production and life. There are many differences in soil characteristics in different regions, which cannot be generalized. Therefore, studying the influence of different soils on leakage signal transmission is of great significance.

Therefore, in this paper, the actual sampled leakage signal is used as the vibration source of numerical simulation through a joint test and numerical simulation, and the propagation model of the acceleration signal of the pipeline leakage vibration is constructed. The attenuation law of the leakage signal propagation along the pipeline is studied. The value of the elastic modulus of the numerical simulation for this problem is discussed using the inversion theory, which further broadens the application field for the numerical simulation in this problem. Furthermore, using this model, the attenuation law of leakage signal with the change of the soil's elastic modulus is studied. This study can provide a basis for the remote detection of leakage signals, provide a reference for the numerical simulation of leakage signal propagation, improve the accuracy of cross-correlation analysis for leakage detection, and enrich the research content of leakage signals.

2. Test Methods

As ductile iron pipes are widely used in water supply networks, they bear the brunt of usage, and as a result the number of leakage incidents of ductile iron pipes is higher than pipes of other materials. It is necessary to further explore the propagation law and mechanism of the leakage acceleration signal of the ductile iron pipeline. Therefore, DN200 buried ductile iron pipeline is used as the test pipeline in this paper, and the pipeline loop, as shown in Figure 1, is composed of other pipelines. The yellow line is the test pipeline, with a depth of 1.2 m; the blue pipe is the other pipeline, with a buried depth of 0 m; the purple box is the road surface; and the red box is the test area. In this test, the water tank is used as the water source, and the variable frequency pump is used as the test pumping and stabilizing equipment. The galvanized steel pipe and PPR pipe form a pipeline loop to drive the water of the pipeline system to return to the water tank, to ensure the stable internal pressure and flow rate in the test pipe section.

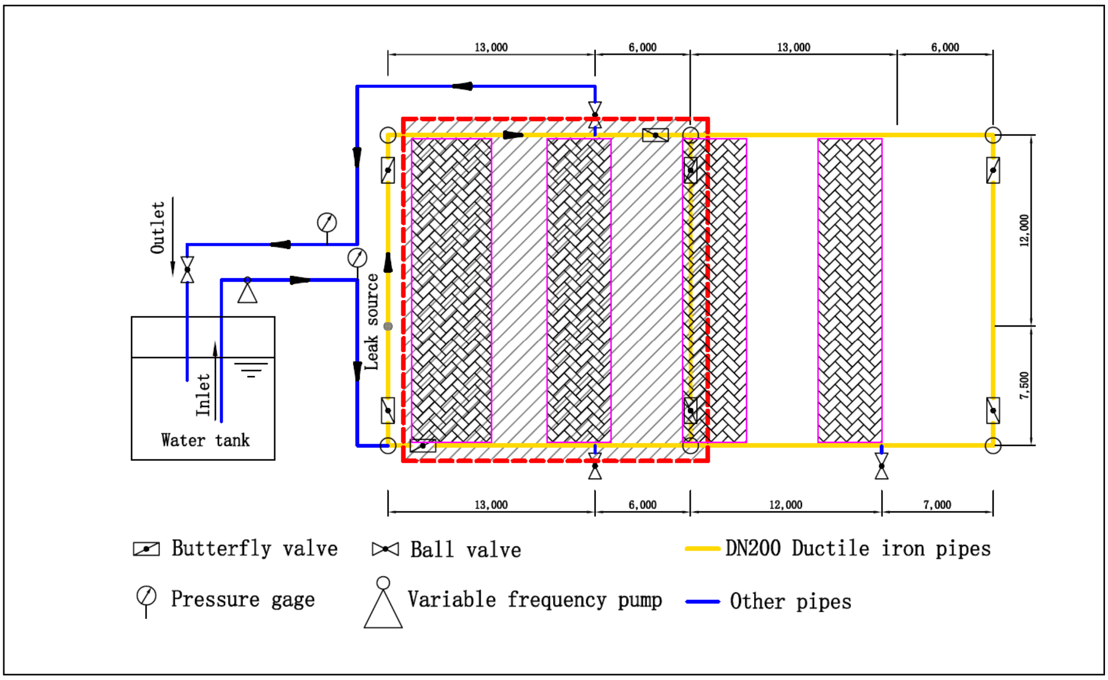

Figure 1. Test layout.

For the test pipe section, make a leak with a diameter of 2.5 mm, and set an internal pressure of 0.6 MPa. The acceleration sensor on the pipe shell is used to simultaneously collect the leakage vibration signals at 0.1 m, 1.0 m, 3.0 m, 6.0 m, and 10.0 m away from the leakage port, and the acquisition frequency is 50,000 Hz to study the propagation characteristics of the leakage vibration acceleration signal along the pipeline. Among them, the sensor with model 1A113E at 0.1 m is named sensor 1, and the sensors with model 1A116E at 1.0 m, 3.0 m, 6.0 m, and 10.0 m are named sensors 2–5, respectively. The sensor parameters are shown in Table 1. As the No. 1 and No. 2 sensors are close to the leak, aluminum foil and plastic film are used to wrap them to avoid signal interference to the sensor when waterdrops fall.

Table 1. Parameters of IEPE piezoelectric acceleration sensor.

Dynamic Indicator	1A113E	1A116E	Physical Parameters	1A113E	1A116E
Sensitivity	50 mV/(m·s^{-2})	10 mV/(m·s^{-2})	Sensor	Ceramics	Ceramics
Amp. Range	±10 g	±50 g	Structural style	Shear	Shear
Linearity	<1%	<1%	Weight	29 g	5.5 g
Lateral Sensitivity	<5%	<5%	Shell material	Stainless steel	Titanium alloy TC4
Resonant Freq	>20 kHz	>35 kHz	Output mode	Side output	Top Output
Resolution	0.00004 g	0.0005 g	Overall dimension	Φ15.5 × 22.5 mm	Φ10 × 22 mm
Axis	Uni-Axial	Uni-Axial	Installation mode	Adhesive	Adhesive

Figure 2 shows the layout of the field test, Figure 3 shows the layout of each sensor, and Figure 4 shows the size of the leak and the leak jet picture during the test.

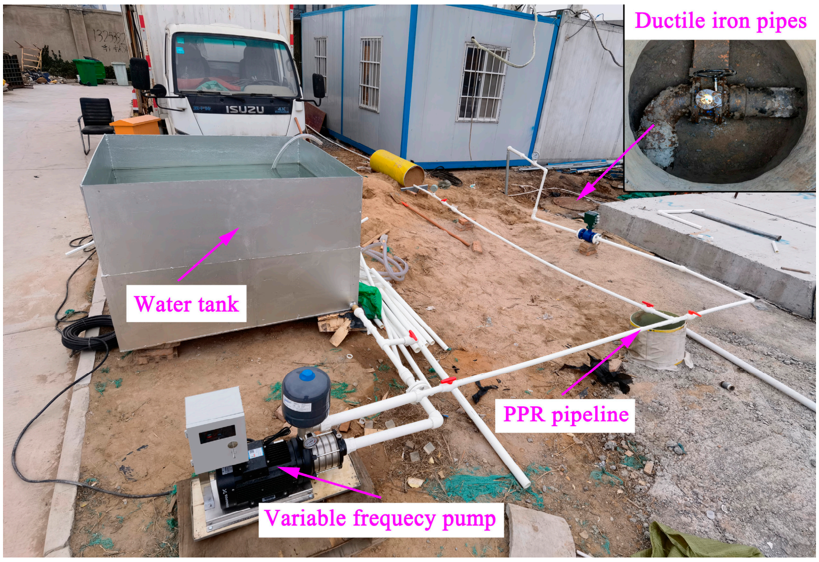

Figure 2. Field equipment layout.

Figure 3. Sensor layout.

Figure 4. Leakage size and jet.

3. Numerical Simulation Method

3.1. Setting of Geometric and Material Models

This article selects COMSOL Multiphysics® 5.6 as a numerical simulation tool. COMSOL uses the finite element method to solve this problem. The physical field of solid mechanics (Formula (1) [29]) is selected. As J.M. Muggleton and M.J. Brennan mentioned in the literature [30] that the energy of a leakage vibration signal will not radiate into water, this paper does not consider the influence of water bodies and establishes a pipe soil coupling model. Since the model is symmetrical, a quarter of it is selected for modeling to save calculation costs. According to the test results, the data collected by the No. 1 sensor (0.1 m away from the leak) is selected as the vibration source of the numerical simulation model. At the left side of the numerical simulation pipe, a 4.5 mm radius leak is selected as the carrier of the vibration source. The finite element model is shown in Figure 5. See Table 2 for the numerical simulation parameters.

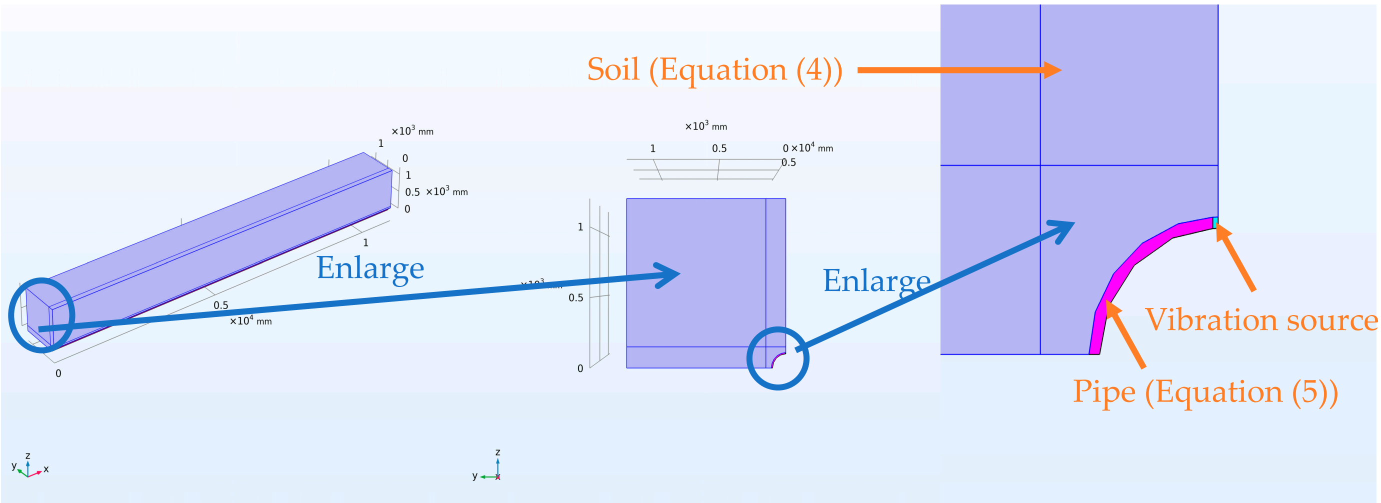

Figure 5. Finite Element Model.

The research has a small deformation problem, and the deformation of the soil and pipe is minimal. Therefore, the linear elastic material model (Formula (2) [29]) is adopted for the pipeline and soil material model, which can ensure accuracy and also save on the calculation cost. The linear elastic material model assumes that the material is homogeneous, continuous, isotropic, perfectly elastic, and has a small deformation. Since the test site is located near Haihang East Road, the physical parameters of the soil are selected from the geotechnical engineering investigation report in Haihang East Road.

Table 2. Table of numerical simulation parameters.

Pipe length	12 m	Inside radius of pipe	0.1 m	Outside radius of pipe	0.109 m
Elastic modulus of pipe	173 GPa	Poisson's ratio of the pipe	0.3	Pipe density	7300 kg/m^3
Soil length	12 m	Soil width	1.2 m	Soil depth	1.2 m
Modulus of compressibility of soil	7.5 MPa	Poisson's ratio of soil	0.3	Soil density	19.8 kg/m^3

In practical engineering problems, soil in different regions affects leakage signal transmission differently. For the elastic model, three physical quantities are generally used to characterize the model: density, Poisson's ratio, and elastic modulus. Generally speaking, the density and Poisson's ratio values for different soils have little difference, while the elastic modulus has an enormous difference. Therefore, this paper uses the elastic modulus to characterize different soils, such as silt and clay, to study the impact of different soil masses on the transmission of leakage signals along the pipeline.

Because the soil is three-phase loose material, when using the elastic model to solve problems about soil, its elastic modulus generally takes different values in small and large deformation problems. Furthermore, the elastic modulus differs from that obtained through a test, generally determined by inversion of the numerical simulation.

For the relationship between the compression modulus and elastic modulus of soil [31], see Formula (3). Generally, the elastic modulus of soil mass is taken as several times the compression modulus. In this paper, the elastic modulus is taken as 1–7 times the compression modulus, respectively, to study the appropriate value of the soil elastic modulus of the numerical simulation model when the leakage signal propagates along the buried pipeline.

This study only considers the transmission of leakage signals in the buried pipeline, so gravity is not considered, and no lateral load is added.

$$\rho\frac{\partial^2\mathbf{u}}{\partial t^2} = \nabla\cdot\mathrm{S} + \mathbf{F}_\mathrm{V} \tag{1}$$

$$\begin{gathered}\mathrm{S} = \mathrm{S}_\mathrm{ad} + \mathbf{C} : \epsilon_\mathrm{el},\ \epsilon_\mathrm{el} = \epsilon - \epsilon_\mathrm{inel}, \epsilon_\mathrm{inel} = \epsilon_0 + \epsilon_\mathrm{ext} + \epsilon_\mathrm{th} + \epsilon_\mathrm{hs} + \epsilon_\mathrm{pl} + \epsilon_\mathrm{cr} + \epsilon_\mathrm{vp} \\ \mathrm{S}_\mathrm{ad} = \mathrm{S}_0 + \mathrm{S}_\mathrm{ext} + \mathrm{S}_\mathrm{q}, \epsilon = \tfrac{1}{2}\left[(\nabla\mathbf{u})^\top + \nabla\mathbf{u}\right], \mathbf{C} = \mathbf{C}(E, v)\end{gathered} \tag{2}$$

$$E = \alpha E_S \tag{3}$$

In the above formulas: ρ is density, kg/m^3; $\mathbf{u}$ is vector displacement, m; t is time, s; S is stress, S_ad is additional stress, S_0 is initial stress, S_ext is external stress, and S_q is viscoelastic stress; where $\mathbf{F}_\mathrm{V}$ is body force per unit deformed volume; ∇ is Hamilton operator; $\mathbf{C}$ is the elasticity tensor, ":" stands for the double-dot tensor product; where ϵ_el is elastic strain, ϵ is total strain, ϵ_inel are all inelastic strains, ϵ_0 is initial strain, ϵ_ext is external strain, ϵ_th is thermal strain, ϵ_hs is hygroscopic strain, ϵ_pl is plastic strain, ϵ_cr is creep strain, and ϵ_vp is viscoplastic strain, 1; where E is Young's modulus, Pa, v is Poisson's ratio, E_S is compression modulus, Pa, α is constant.

In this paper, only the elastic strain is considered, but inelastic strains are not considered. In other words, ϵ_inel = 0.

3.2. Constraint Setting

Since this model only takes a part of the whole pipe network and soil, it adopts a quarter symmetric model. The surface soil is exposed to air. According to the coordinate system shown in Figure 5 and the right-hand rule, the constraint conditions of each interface are as follows.

The symmetry planes allowing normal free displacement (Formula (4) [29]) include: (a) at X = 0, a negative X plane of soil and pipe; (b) at Y = 0, the negative Y plane of the soil; (c) at Z = 0, the negative Z plane of soil and pipe.

An asymmetrical plane with a normal displacement of 0 (Formula (5) [29]) is: at Y = 0, the negative Y plane of the pipe.

As the actual pipeline is in infinite soil, the leaked elastic wave is finally absorbed by the surrounding soil. Nevertheless, the finite element model only selects part of the soil and pipeline for simulation, and there will be reflected wave interference at the interface. Therefore, the low reflection interface (Formula (6) [29]) is set to absorb elastic waves as much as possible and avoid the impact of reflected waves on numerical accuracy, which include: (a) at Y = 1.2 m, the positive Y plane of the soil; (b) at X = 12 m, the positive X plane of soil and pipe.

The actual soil and air interface can be considered unrestrained, so the positive Z plane is the free interface at Z = 1.2 m.

$$\mathbf{u}\cdot\mathbf{n} - u_n = 0 \tag{4}$$

$$\mathbf{u}\cdot\mathbf{n} = 0 \tag{5}$$

$$\begin{gathered}\sigma\cdot\mathbf{n} = -\mathbf{d}_\mathrm{im}\tfrac{\partial\mathbf{u}}{\partial t} \\ \mathbf{d}_\mathrm{im} = \mathbf{d}_\mathrm{im}(\rho, c_\mathrm{s}, c_\mathrm{p})\end{gathered} \tag{6}$$

where $\mathbf{n}$ is a normal vector, u_n is normal displacement, σ is stress, Pa; $\mathbf{u}$ is vector displacement, m; $\mathbf{d}_{\mathrm{im}}$ is mechanical impedance; c_{p} and c_{s} are the speeds of the pressure; and shear waves in the material, m/s.

3.3. Probe, Mesh, and Solver Settings

The probe is set to detect the change of the vibration acceleration at various places on the pipe.

The structured mesh is mapped and constructed, and the mesh size changes are constructed through a geometric series so that the mesh near the pipeline is dense and the mesh far from the pipeline is sparse to achieve higher computing efficiency. Finally, the free tetrahedron mesh is adopted around the pipe for densification. In order to accurately analyze the elastic wave when the vibration signal propagates on the pipeline, 6–8 mesh cells should be guaranteed for each wavelength [32]. Assuming that the minimum wavelength of the elastic wave is λ_{min}, there is:

$$\lambda_{\mathrm{min}} = c_0 / f_{\mathrm{max}}. \tag{7}$$

However, the frequency of the test acquisition signal is 50,000 Hz. According to the Nyquist frequency, f_{max} is 25,000 Hz, and the pressure wave velocity c_0 of the ductile iron pipe is 5648 m/s, so the mesh size should not be more than $\lambda_{\mathrm{min}}/8 = 28\ mm$. Therefore, the maximum unit size of the pipe selected in this study is 25 mm. Each mesh size is less than 25 mm, which meets the requirements. Experiments verify that the high-frequency signal attenuates rapidly and the low-frequency signal continues to propagate. Therefore, mesh of this size has fully met the requirements of signal propagation for low-frequency signals. The model mesh distribution is shown in Figure 6.

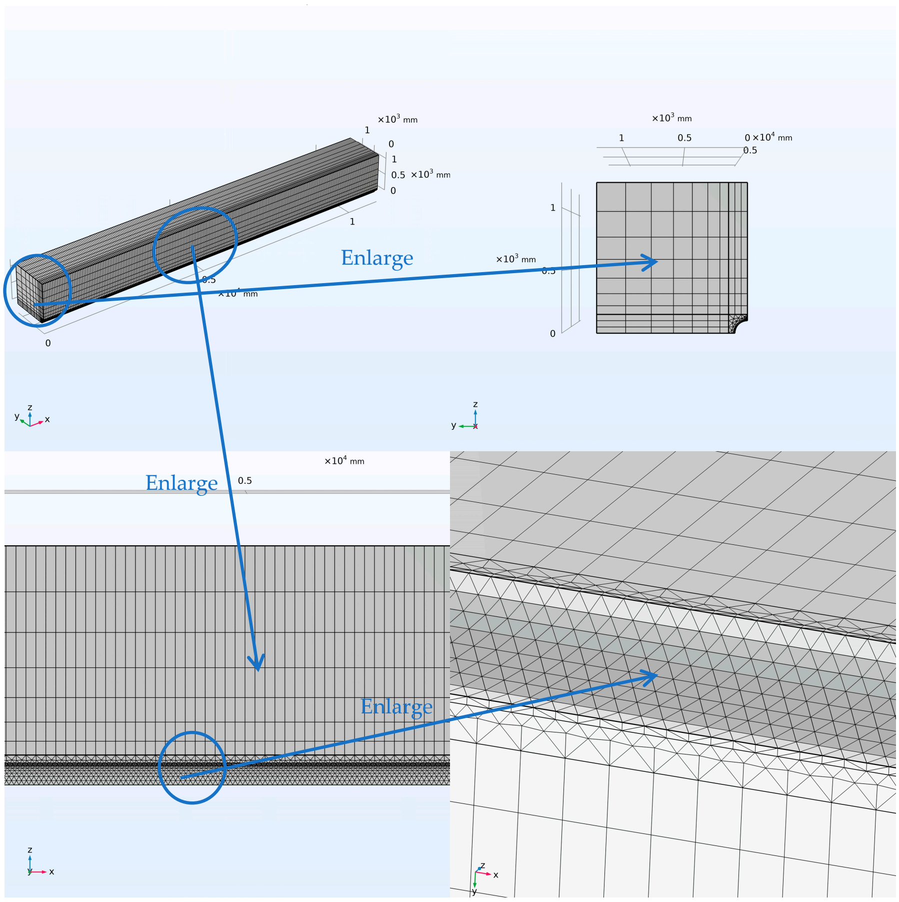

Figure 6. Mesh and its details.

The calculation time is set to [0,0.00002,0.11]s to ensure that the time step is consistent with the step of the signal collected by test sensor No. 1. The start time is 0 s, time step is 0.00002 s, and end time is 0.11 s. The calculation method is the fully coupled generalized α method, and the fixed step size is adopted for the calculation. The calculated degree of freedom is 527,338.

4. Analysis of Test Data

4.1. Time Domain Analysis of Leakage Signal

As shown in Figure 7, the acceleration signals are collected at 0.1 m, 1 m, 3 m, 6 m, and 10 m away from the leakage point in the test. The data of each sensor is counted, and the data interval and amplitude mean value collected by each sensor is obtained in Table 3. Each signal vibrates to-and-fro. With the distance from the leakage source increasing, the vibration energy is gradually dissipated into the surrounding space, and the vibration acceleration amplitude is gradually reduced.

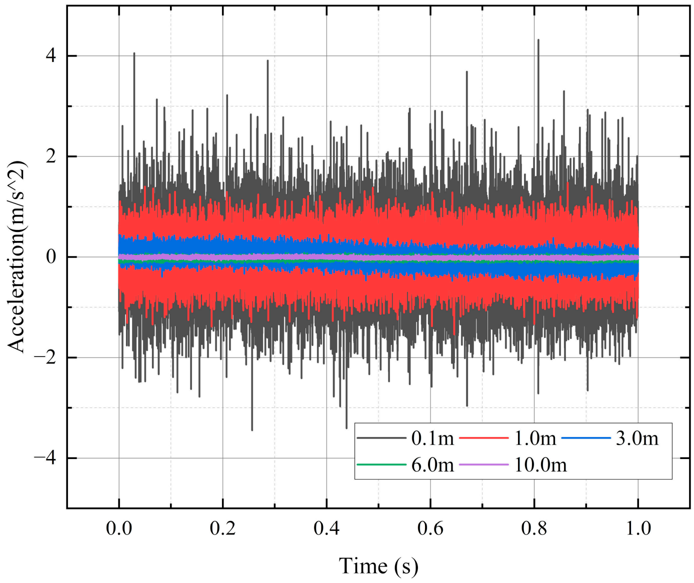

Figure 7. Time domain diagram of vibration signals collected by each sensor in the test.

Table 3. Data interval and mean value of test acquired signal.

Distance (m)	0.1	1	3	6	10
Acceleration interval (m/s^2)	[−3.447, 4.321]	[−1.539, 1.476]	[−0.503, 0.477]	[−0.131, 0.091]	[−0.076, 0.063]
Average amplitude (m/s^2)	0.47394	0.28177	0.10346	0.03105	0.01566

The variation of amplitude with distance is shown in Figure 8. The fitting curve is an exponential function: $y = A_1 e^{-x/t_1} + y_0$, where A_1, t_1, and y_0 are parameters, $R^2 = 0.99954$. In terms of transmission distance, the leakage signal attenuates faster in the early stage and slows down in the late stage. The amplitude at the leakage source is expressed by y-intercept $y(0) = A_1 + y_0$ (A_1 and y_0 are parameters). The magnitude of the vibration amplitude at the vibration source is mainly determined by the pipe material, internal pressure, leakage size and shape, and the environment around the pipe. That is, two parameters can be used as the comprehensive digital expression of the above factors to a certain extent. The attenuation rate of the vibration signal along the pipeline is the function's derivative, represented by A_1 and t_1. This parameter characterizes the influencing factors, such as pipeline materials and soil around the pipeline, as the attenuation rate. The pipe material has been determined for the specific pipe and will not be discussed here. However, the influence of different soils on the signal attenuation law and its mechanism is still unclear and needs further study.

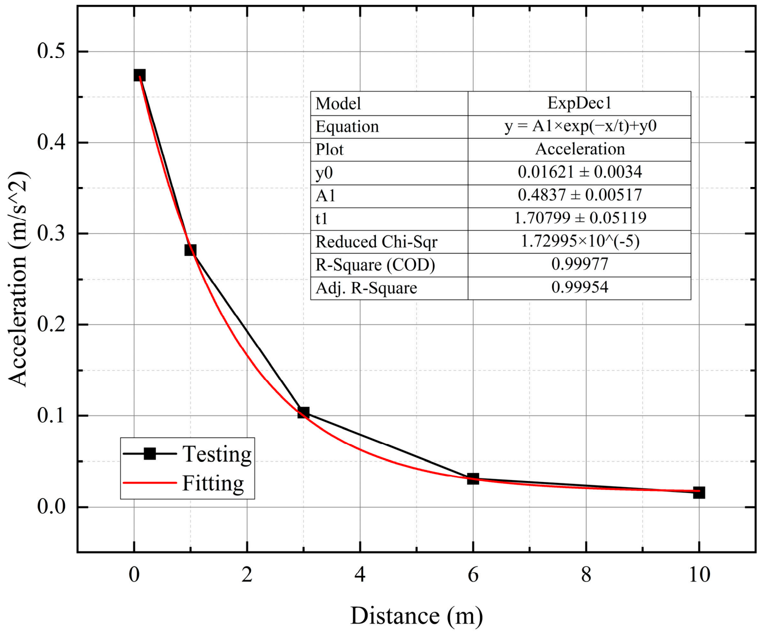

Figure 8. Variation relation and fitting diagram of test leakage signal amplitude and distance.

4.2. Frequency Domain Analysis of Leakage Signal

The 25,000 Hz is divided into three parts: the first frequency band 1–8333 Hz, the second frequency band 8334–16,666 Hz, and the third frequency band 16,667–25,000 Hz.

Figure 9 shows the frequency domain image of the acceleration signal acquired in the test. At 0.1 m, the vibration signal fills the whole frequency domain. The signal is composed of multiple peaks, which are more distributed in high-frequency, especially in the third frequency band. At 1 m, the signal is lost in the whole frequency band. Among them, third band has the most signal loss, and the decline of magnitude is the most obvious. The basic rule is that the higher the frequency, the greater the signal loss. That is to say, in the process of the vibration signal propagating along the pipeline, the higher the frequency of the signal, the more times of vibration per unit time, and then the greater the heat loss. More energy is converted into heat energy, and the faster the signal loss of this frequency is. At 3 m, as the distance further increases, the vibration signal energy is increasingly more converted into the heat energy of the pipeline and the surrounding soil, and each frequency has a large loss. At 6 m, the signal is further lost. Except for individual peaks, the characteristics of many peaks have gradually disappeared, and the frequency distribution is gentler than before. The magnitude of peak frequency and the surrounding frequency are gradually approaching, with no peaks protruding, and some peaks have disappeared. At 10 m, except for the first frequency band, the peaks of other frequencies tend to disappear and cannot be distinguished on the spectrogram. That is to say, the high-frequency signal greater than 8333 Hz has lost the significance of obtaining effective information in remote detection and only brings noise signals.

Calculate each frequency band's energy and total energy using Formula (8) and draw the curve of the energy proportion of each frequency band changing with the leakage distance, as shown in Figure 10.

$$P_f = 2\left(\frac{1}{T_s}\frac{\sum X_f}{F_s}\right)^2 \tag{8}$$

where P_f is the total energy of the signal in the frequency domain; T_S is the sampling time, and 1 s is taken for the test data; F_S is the sampling frequency, and 50,000 Hz is taken for the test data; X_f is the Fourier transform magnitude of frequency f.

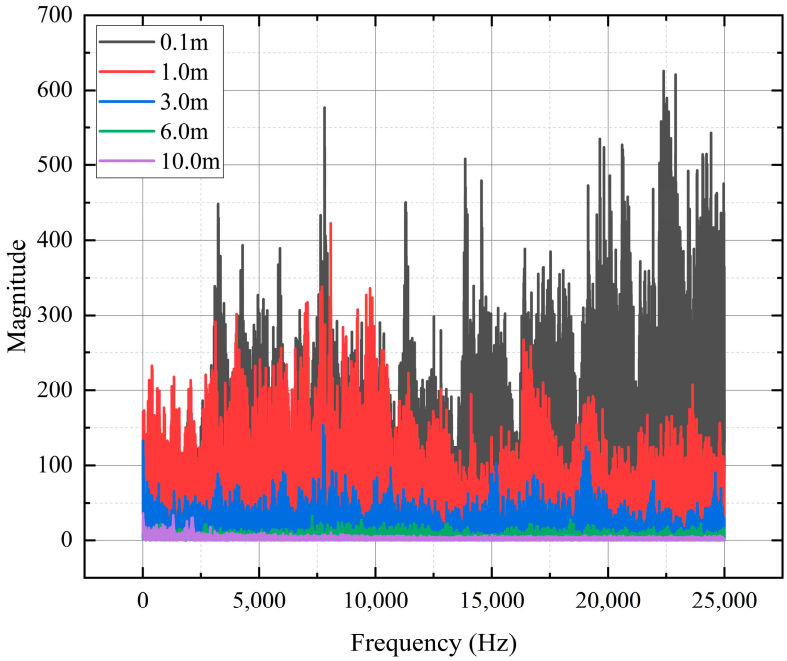

Figure 9. The frequency spectrum of vibration signals collected by each sensor in the test.

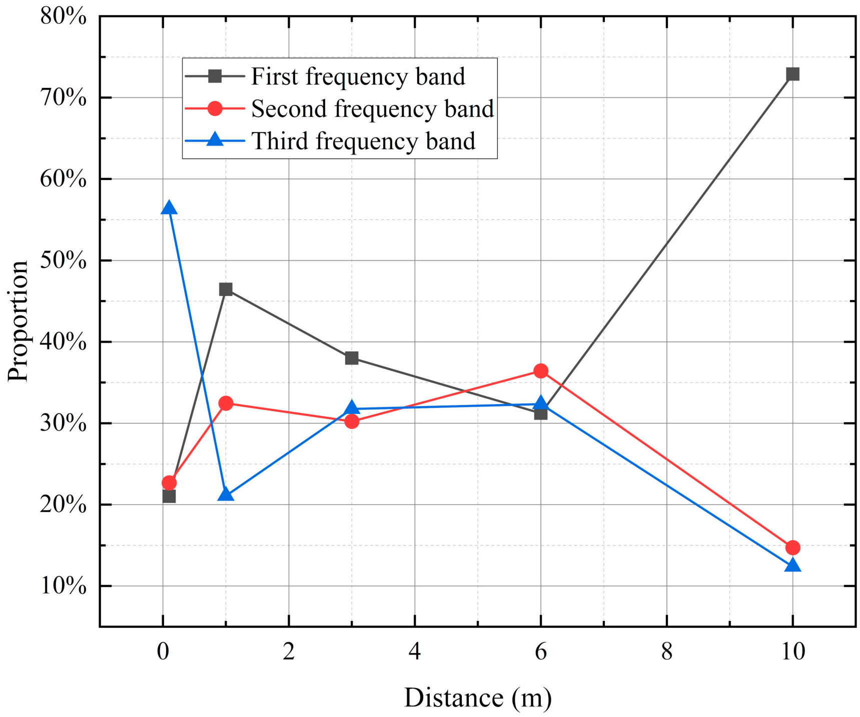

Figure 10. The change of energy proportion curve of each frequency band with leakage distance.

At 0.1 m, the energy ratio of the first, second, and third frequency bands is 21%, 23%, and 56%, respectively. The energy proportion of the third frequency band has obvious advantages, and the signal is mainly a high-frequency signal. At the stage of 0.1 m–1 m, the proportion of energy in the third frequency band rapidly drops to 21%, indicating that the energy in the high-frequency part of the signal decayed rapidly within a short distance from the leakage point. In the 0.1 m–6 m stage, the proportion of energy in each frequency band tends to be consistent, which indicates that the distribution of signals in the whole frequency band is gradually averaged, and the peak characteristics of signals gradually disappear. At 6–10 m, the proportion of energy in the first frequency band rapidly rises to 73%. The proportion of the other two frequency bands drops below 15%, indicating that the high-frequency signal has been attenuated. Only the low-frequency signal continues to propagate.

In general, when the vibration signal propagates along the pipeline, it is shown that with the increase of distance, the signal strength of each frequency weakens on the whole, the high-frequency signal attenuates faster than the low-frequency, and its peak characteristic disappears earlier. When detecting the leakage signal from a distance, the signal greater than 8333 Hz has been mixed with the noise, so effective information cannot be obtained. Using sensors with smaller frequency responses but higher sensitivity to detect leakage signals at a longer distance is more reasonable and accurate.

4.3. Group Velocity Analysis

When the correlation analysis method detects the pipeline leakage, the time difference between the two sensors to obtain the signal is used to infer the leakage location. Therefore, once the propagation speed of the leakage signal cannot be accurately obtained, the detection accuracy will not be discussed. Thus, the acquisition of the propagation speed of the leakage signal is very important. The essence of signal propagation is the propagation of energy, and in elastic media, energy velocity and group velocity are equivalents [33]. Therefore, it is significant to obtain the group velocity. In this study, the vibration signal generated by an instantaneous jet is used as a reference to calculate the group velocity of the test.

Figure 11 shows the signals collected by sensors 1 and 5 for this jet phenomenon. The calculation of group velocity rules are as follows: in the 0–0.02 s time interval, which can reflect the amplitude of the "noise" signal, 10 times the average amplitude in this interval is used as the standard. To remove certain randomness, the speed at which the signal amplitude reaches no less than the amplitude standard for the second time is taken as the group velocity. After calculation, select T_1 = 0.0375 s for sensor 1, T_2 = 0.04816 s for sensor 5, and take the distance between two sensors S = 9.9 m, then the group velocity $v_q = S/(T_2 - T_1) = 929\ m/s$.

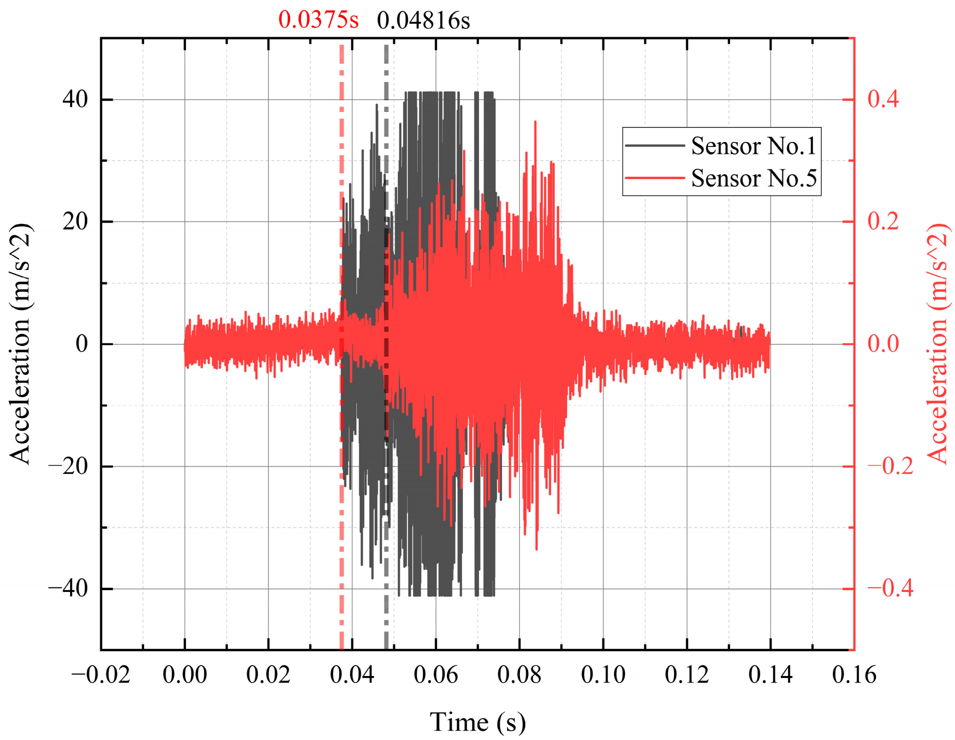

Figure 11. The time the jet signal appears in sensors 1 and 5.

The physical parameters of the pipeline in Table 2 can be obtained and can be calculated by Formula (9) [29]:

$$\begin{aligned} c_{\mathrm{p}} &= \sqrt{\frac{E(1-\nu)}{\rho(1+\nu)(1-2\nu)}} \\ c_{\mathrm{s}} &= \sqrt{\frac{E}{2\rho(1+\nu)}} \end{aligned} . \tag{9}$$

The pressure-wave speed c_{p}= 5648 m/s, and the shear-wave speed c_{s}= 3019 m/s, differ from the group velocity calculated in this study. It shows that the existence of surrounding soil does significantly affect the transmission group velocity of the pipeline vibration signal and plays a role in reducing it. Therefore, studying the influence of different soils on the group velocity of pipeline leakage signals is of great value.

5. Numerical Simulation Data Analysis

The part with Z > 0 is mirrored, and the propagation of the numerical simulation acceleration signal in the soil and pipeline is shown in Figure 12. It should be noted that to see the image of the propagation and distribution of the acceleration signal more clearly, this figure limits the display range of the legend. During the influence of its own and soil damping, the acceleration signal attenuated rapidly in the propagation process in the pipeline's length direction. One part of the acceleration signal was dissipated in space, and the other continued to propagate along the pipeline. Moreover, the amplitude of acceleration near the pipeline is always the largest in the cross-section direction in this figure. As shown above, signal radiation is characterized by the superposition of cylindrical and spherical waves.

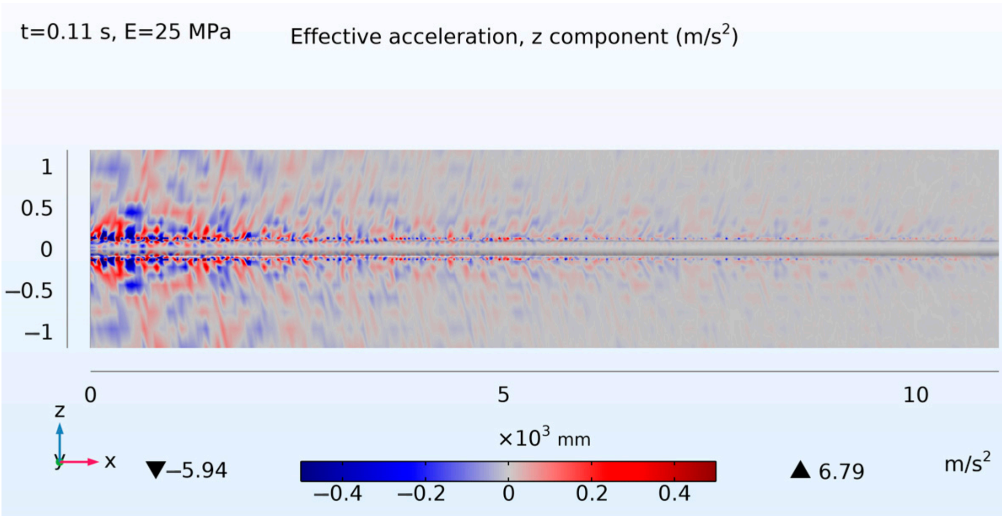

Figure 12. Propagation of acceleration signal in numerical simulation.

5.1. Determination of Elastic Modulus in Numerical Simulation

For numerical simulation, the elastic modulus is 1–7 times the compression modulus, as shown in Table 4, to study the value of the soil elastic modulus of the numerical simulation model when the leakage signal propagates along the buried pipeline.

Table 4. Working conditions of numerical simulation.

Working conditions	1	2	3	4	5	6	7	8
E (MPa)	7.5	15	22.5	25	30	37.5	45	52.5

Since the No. 1 sensor is very close to the leakage point, the sensor's signal is used as the source of the leakage signal of the numerical simulation model. However, the sensor is a certain distance from the leak. The vibration signal attenuates violently at the initial stage, so the signal cannot fully replace the leak source signal in amplitude. Therefore, the signal is processed as follows to fully replace the vibration signal of the leakage source at X = 0 m. Based on the vibration amplitude at 0.1 m during the test, all the data collected by the numerical simulation probe are multiplied by the amplification factor β to make it equal to the amplitude of the signal collected by the No. 1 sensor at X = 0.1 m, as shown in Formula (10):

$$\beta = 0.47394/a_{p,x=0.1},\ a = \beta a_p, \tag{10}$$

a is the acceleration signal used in actual data processing; a_p is the acceleration signal collected by the probe during numerical simulation; and β is the amplification factor.

As the attenuation law of each working condition is relatively consistent, only three groups of data are taken for analysis to facilitate observation. As shown in Figure 13, the E = 25 MPa curve is the closest to the test curve. However, in the test, the first 1 m of the pipe is semi-exposed to the air, as shown in Figure 14. Therefore, it does not conform to the condition that the pipe is completely buried in the soil 1.2 m deep during simulation. Therefore, for the numerical simulation model, under the condition of E = 25 MPa, remove the soil of the first 1 m to obtain a modified pipe model that is completely exposed in the first 1 m. The comparison between the data of the two models and the test data is shown in Figure 15.

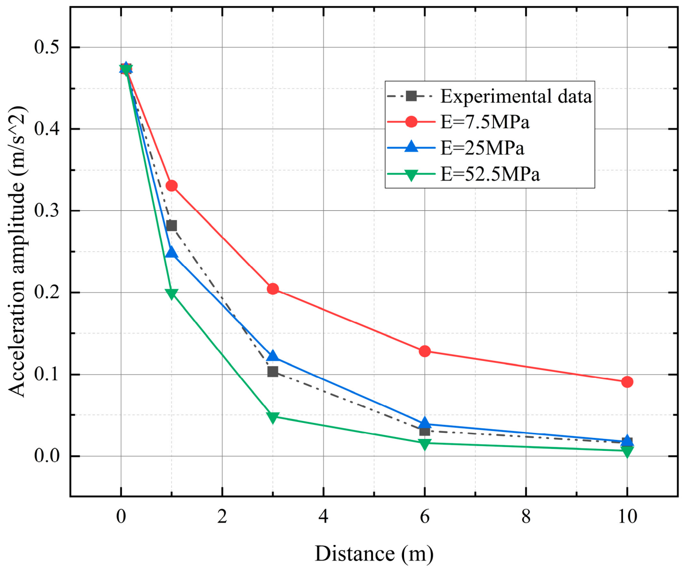

Figure 13. Comparison of acceleration amplitude attenuation curves with different elastic moduli and test curves.

The original model has soil absorbing vibration energy at 0–1 m, so the amplitude decreases faster. Since the first 1 m of the modified model is completely exposed, the attenuation speed is relatively small. The test situation is that the first 1 m pipe is half exposed to air and half buried in the soil. Therefore, in terms of data, the amplitude change curve of the test is perfectly between the curves of the two models. Furthermore, the three curves intersect at a point of about 2.2 m. This data fully and effectively proves the correctness and reliability of the numerical simulation model. It also shows that it is appropriate that the elastic modulus of the soil around the pipe, from the numerical simulation model, is 3.3 times its compressive modulus in detecting the vibration acceleration signal of water pipeline leakage.

In fact, the pipeline is generally buried in the soil during testing, so the data of the original model are used for subsequent analysis.

Figure 14. The first 1 m of the pipe in the test is semi-exposed to the air.

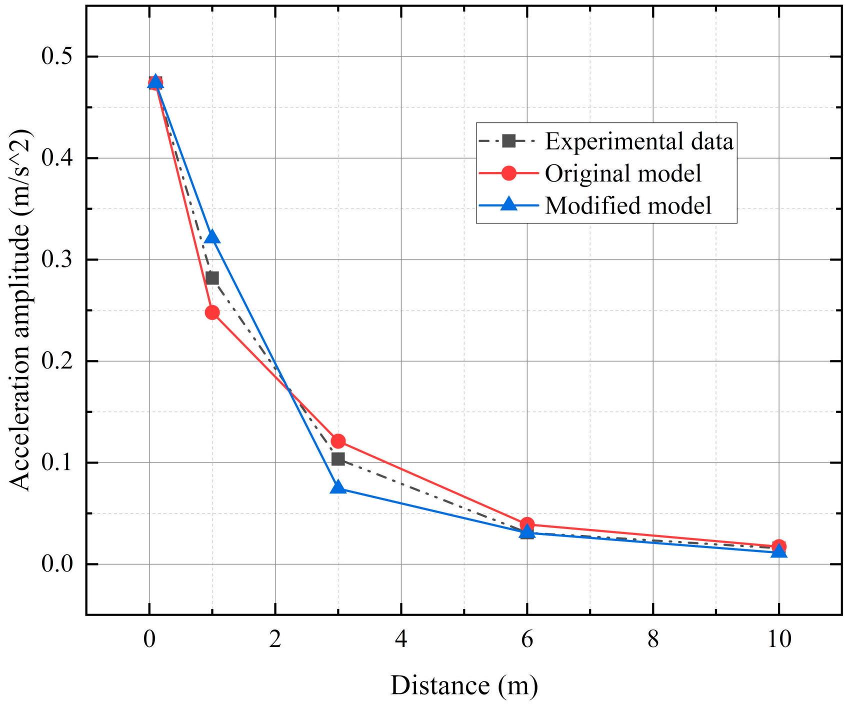

Figure 15. Comparison of the original model, modified model, and test data.

5.2. Variation Rule of Four Parameters of Propagation Rule

Since the fitting function of the signal amplitude attenuation curve of the test data is $y = A_1 e^{-x/t_1} + y_0$, the four parameters and R^2 obtained by fitting the function to each working condition of the numerical simulation are shown in Table 5.

Table 5. Values of fitting function parameters under various working conditions of numerical simulation.

E (MPa)	7.5	15	22.5	30	37.5	45	52.5
y_0	0.09383	0.05271	0.0355	0.01891	0.01368	0.0142	0.01315
A_1	0.39056	0.43681	0.45781	0.47862	0.4918	0.49965	0.50712
t_1	2.25321	1.90027	1.64796	1.50967	1.3874	1.14533	1.01866
$y_0 + A_1$	0.48439	0.48952	0.49331	0.49753	0.50548	0.51385	0.52027
R^2	0.99608	0.9956	0.99321	0.99319	0.99877	0.99873	0.99917

Draw Table 5 as shown in Figure 16.

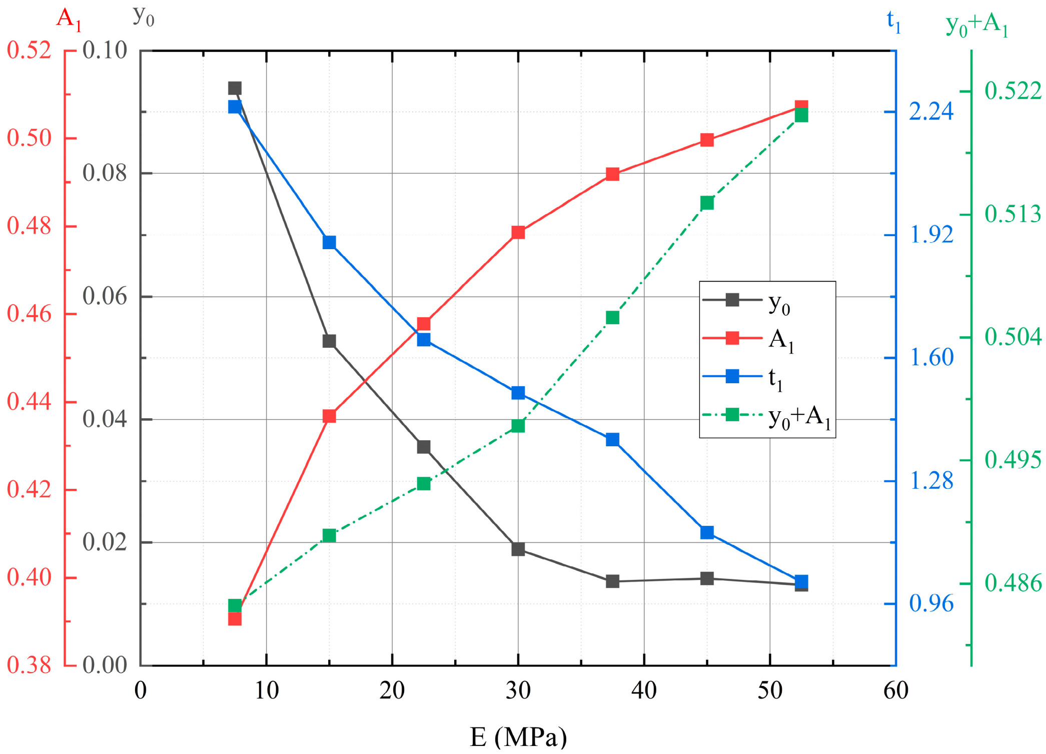

Figure 16. Changing rule of four parameters of signal attenuation fitting curve with elastic modulus.

y_0 and t_1 decrease as the elastic modulus increases, while A_1 increases. $y_0 + A_1$ represents the intercept of y, which increases with the increase of the elastic modulus. At 0.1 m, because the above data have been adjusted by Formula (10), the values at 0.1 m are equal. The larger the y-intercept is, the greater the signal attenuation is in the 0–0.1 m range. The greater the elastic modulus, the greater the attenuation speed of the vibration signal in the range of 0–0.1 m. The change of attenuation velocity of the vibration signal with the elastic modulus in this interval is linear. The parameters of the fitting curve of A_1, t_1, y_0, and $y_0 + A_1$ with the change of the elastic modulus are shown in Table 6.

Table 6. Fitting curve parameters of each parameter value changing with elastic modulus.

Parametric function	A_1	t_1	y_0	$y_0 + A_1$
Function Type	$A_1 = A_2e^{-E/t_2} + y_1$	$t_1 = a_1E + b_1$	$y_0 = A_3e^{-E/t_3} + y_2$	$y_0 + A_1 = a_2E + b_2$
A_i	−0.18671	/	0.16281	/
t_i or a_i	19.08312	2.3338	11.28785	0.47655
y_i or b_i	0.51792	−0.02607	0.01015	8.02×10^{-4}
R^2	0.99741	0.9721	0.99518	0.97995

Table 6 above can be converted into Formula (11) to obtain the relationship between the amplitude attenuation law of pipeline leakage vibration signal and distance, and soil elastic modulus.

$$y(x, E) = (A_2 e^{-E/t_2} + y_1) e^{-x/(a_1 E + b_1)} + (A_3 e^{-E/t_3} + y_2) \tag{11}$$

The variation law of the attenuation rate y_a of the amplitude attenuation curve is shown in Formula (12) by using Formula (11). The variation of the attenuation rate with the elastic modulus and distance is plotted as shown in Figure 17, where E is the parameter variable.

$$y_a = -\frac{dy(x, E)}{dx} = \frac{A_2 e^{-E/t_2} + y_1}{a_1 E + b_1} e^{-x/(a_1 E + b_1)} \tag{12}$$

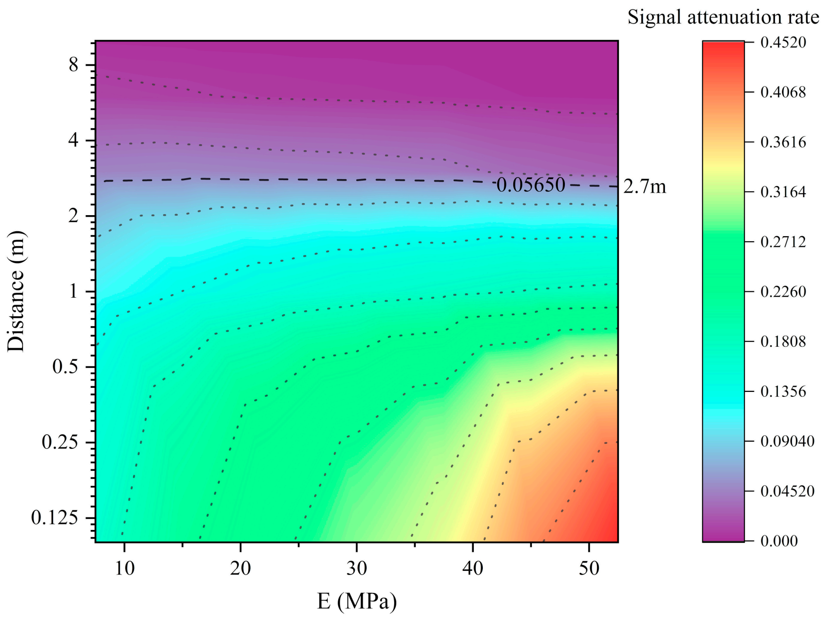

Figure 17. Isogram of signal attenuation rate versus elastic modulus and distance.

In Figure 17, a large value attenuation rate indicates fast attenuation and steep amplitude attenuation curves. A small value means slow attenuation, and the amplitude curve is relatively gentle. The attenuation rate for soils with any elastic modulus generally decreases with the distance increase. For different locations, in the range of 0.1–2.7 m, the attenuation rate increases with the elastic modulus increase. The attenuation rate decreases at 2.7–10 m with the elastic modulus increase. That is to say, the amplitude of the leakage signal attenuates rapidly in the near place and slowly in the far place.

Combined with the previous discussion on the 0–0.1 m interval, the following conclusions can be drawn: (a) The attenuation curve of the acceleration signal amplitude of the pipeline leakage vibration is a function of distance and soil elastic modulus. The signal amplitude generally decreases with the increase of distance. For the same leakage signal, the amplitude of the vibration signal corresponding to soil with a high elastic modulus is always smaller at the same location. (b) For the same soil, the attenuation rate of the signal always decreases with the increase of distance. That is, the attenuation nearby is faster, and the attenuation far away is slower. (c) At the same location, from 0–2.7 m, the larger the elastic modulus of soil mass is, the greater the corresponding signal attenuation rate is. At 2.7–10 m, the smaller the elastic modulus of soil, the greater the corresponding signal attenuation rate. (d) The increase or decrease of the same value of elastic modulus of soil with a high elastic modulus has less influence on the signal than the increase or decrease of the same value of elastic modulus of soil with a low elastic modulus. That is, the attenuation of the vibration signal is more insensitive to the change of the elastic modulus of soil with a high elastic modulus.

5.3. Frequency Domain Analysis of Numerical Simulation Data

Because the sensor is far from the leak during actual detection, this paper selects the result at 10 m of numerical simulation as the object of frequency domain analysis. The signal spectrum at 10 m of the pipe under each elastic modulus is plotted as shown in Figure 18.

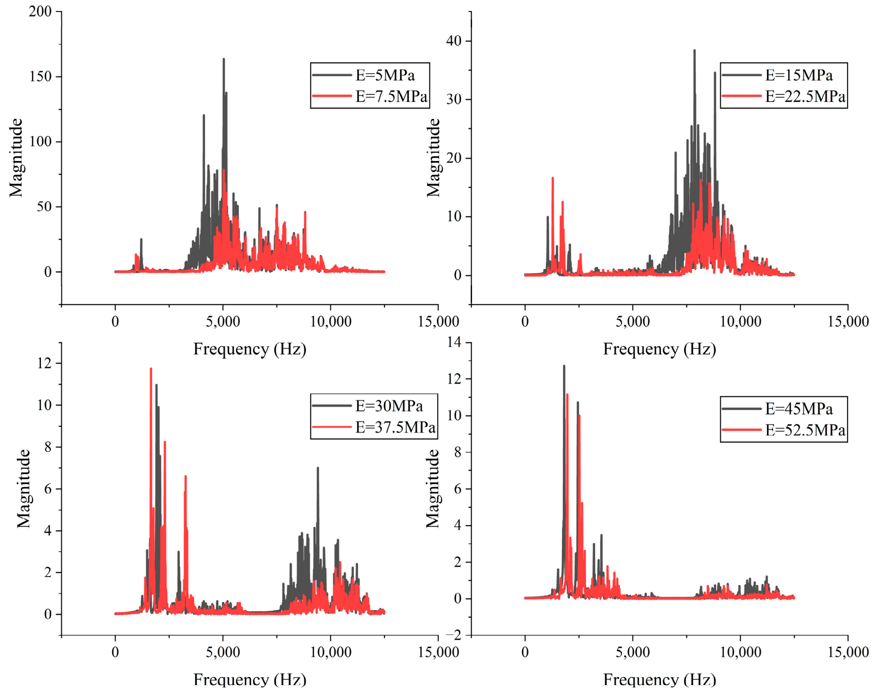

Figure 18. The spectrum of the signal at 10 m under each elastic modulus.

On the whole, with the increase of the elastic modulus, the magnitudes accumulated at the same time decreased. It shows that the expansion of the elastic modulus increases signal attenuation. The signal corresponding to each elastic modulus can be divided into two peaks representing the low-frequency and high-frequency parts. The two peaks for the image with E = 5 MPa are 1200 Hz and 5035 Hz, respectively. For E = 52.5 MPa, the two peaks are 1954 Hz and 11,261 Hz, respectively, and the first and second peaks have both shifted to the right compared with E = 5 MPa. At the same time, with the increase of the elastic modulus, the relative magnitude of the first peak gradually increases, and the relative volume of the second peak gradually decreases. This phenomenon reflects that the soil with different elastic moduli has different energy absorption capacities for different frequency signals.

In general, the soil with a high elastic modulus absorbs more energy, which reduces the magnitudes of different frequencies of signals. Still, its absorption capacity for different frequencies of signals is different. The higher the elastic modulus of the soil, the stronger the energy absorption capacity of the high-frequency part of the signal, making its low-frequency component more significant.

5.4. Relationship between Group Velocity and Elastic Modulus of Soil

During numerical simulation, since the pipeline has no vibration in the initial state, the only vibration source is from X = 0, so the time of the first signal received at 10 m can be used as the basis for calculating the signal transmission speed. The signal at 10 m under each working condition is shown in Figure 19.

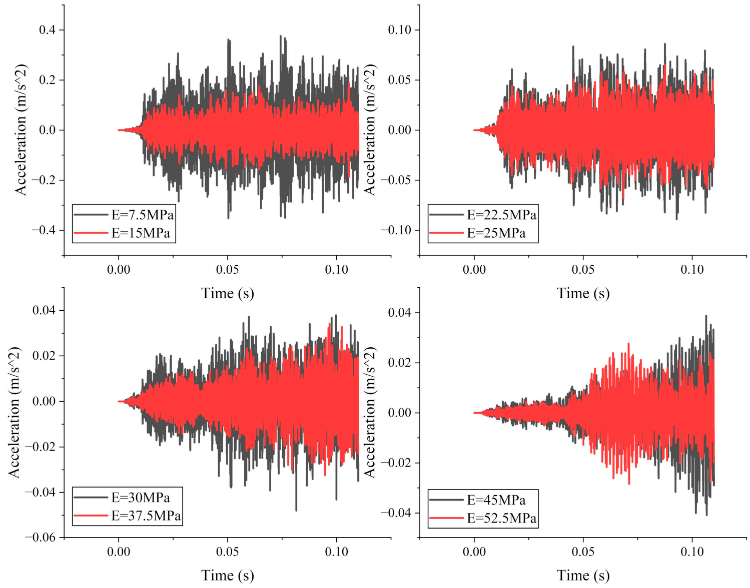

Figure 19. Acceleration signal at 10 m under various working conditions.

Due to the dispersion of leakage signals during transmission [34], signals with different frequency components arrive at 10 m at different times. That is, the speed of signal transmission is related to its frequency. The group velocity equals the energy transfer velocity, so the group velocity should be calculated using the amplitude arrival time. The calculation rules are as follows: since signals with different frequency components have reached 10 m in the 0.07–0.11 s time interval, which can reflect the amplitude of the whole signal, 1/3 of the average amplitude in this interval is used as the standard, and to remove certain randomness, the speed at which the signal amplitude reaches the amplitude standard for the second time is taken as the group velocity.

As shown in Figure 20, the group velocity of the vibration signal is maintained at about 925 m/s within 7.5–37.5 MPa. This velocity is very close to the group velocity of 929 m/s calculated in the test, which fully proves the correctness of the numerical simulation model. Within 37.7–52.5 MPa, the group velocity of the vibration signal decreases greatly, which is 645 m/s at 52.5 MPa.

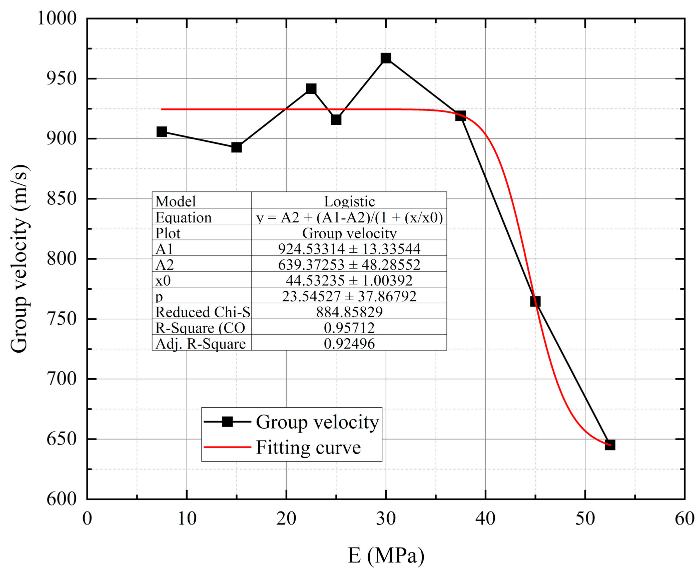

Figure 20. Relationship between soil elastic modulus and group velocity of pipeline leakage vibration signal.

The working conditions with the elasticity of 7.5 MPa, 25 MPa, and 52.5 MPa are selected to analyze the amplitude of the vibration signal before 0.006 s. The signal amplitudes of E = 25 MPa and E = 52.5 MPa have been amplified two and five times, respectively.

As shown in Figure 21, the group velocity of the pipeline leakage vibration signal is different for soils with a different elastic modulus. The wave packet of the signal reaches 10 m in about 0.01 s–0.015 s. However, many frequency components have arrived as early as about 0.002 s. That is, the phase velocity of these frequency components is faster than the group velocity, and this phenomenon exists for soils with a different elastic modulus. According to Figure 18, this part of the signal is the high-frequency signal because only the low-frequency signal is left for the pipeline vibration signal corresponding to the soil with a high elastic modulus, and its group velocity is small. However, currently, the phase velocity of some frequency signals is relatively large, so the signals in this part are high-frequency signals. That is, the phase velocity of a high-frequency signal is relatively large, while that of the low-frequency signal is relatively small.

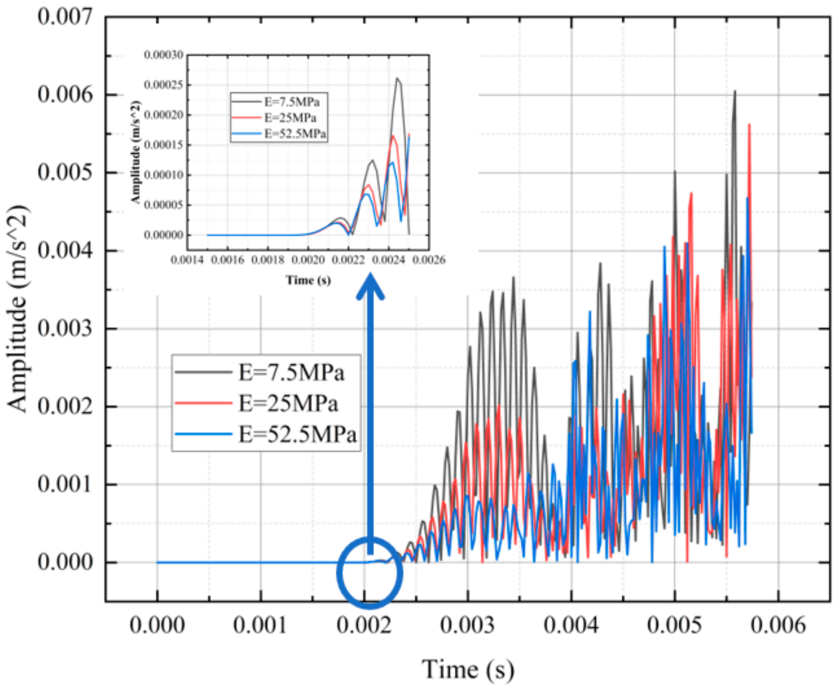

Figure 21. Analytical diagram of signal propagation speed.

In general, the group velocity of the pipeline leakage vibration signal is affected by the elastic modulus of the surrounding soil. When the elastic modulus of soil is within the range of 7.5–37.5 MPa, the group velocity is about 925 m/s. When the elastic modulus of soil is greater than 37.5 MPa, its group velocity will decrease significantly. The reason is that for soil with a high elastic modulus, its signal absorption capacity for high-frequency components is stronger, so its signal is mainly composed of low-frequency components. While the phase speed of the low-frequency part of the leakage signal is slower than the high-frequency part, the group speed of the leakage signal corresponding to the soil with a high elastic modulus will be slower.

6. Conclusions

In this paper, the propagation characteristics of the water pipeline leakage signal in the test are studied by combining the research of the test and numerical simulation. A solution to the problem of soil physical parameters is proposed in a numerical simulation. The influence rule and mechanism of the elastic modulus of soil covered with the pipeline on the propagation characteristics of the acceleration signal of pipeline leakage vibration are discussed, such as the attenuation rule of time domain signal amplitude, frequency distribution rule in the frequency domain, and signal propagation group velocity. Research findings:

- The attenuation curve of the acceleration signal amplitude of pipeline leakage vibration is a function of distance and soil elastic modulus, which conforms to the $y(x,E) = (A_2e^{-E/t_2} + y_1)e^{-x/(a_1E+b_1)} + (A_3e^{-E/t_3} + y_2)$ relationship. On the whole, there are the following rules: (a) In general, the signal amplitude decreases with the increase of distance and, for the same leakage signal at the same location, the vibration signal amplitude of soil with a high elastic modulus is always smaller; (b) For the same soil, the attenuation rate of the signal always decreases with the increase of distance. That is, the attenuation nearby is faster, and the attenuation farther away is slower; (c) For the same location: at 0 m–2.7 m, the greater the elastic modulus of soil mass, the greater the corresponding signal attenuation rate; and at 2.7–10 m, the smaller the elastic modulus of soil mass, the greater the corresponding signal attenuation rate. (d) The attenuation of the vibration signal is more insensitive to a change of the elastic modulus of soil with a high elastic modulus than low.
- When the vibration signal propagates along the pipeline, the signal strength of each frequency component decreases as a whole with the increase of distance. A high-frequency signal attenuates faster than a low-frequency signal, and its peak value disappears earlier. When detecting the leakage signal from a distance, the signal greater than 8333 Hz has been mixed with noise, so effective information cannot be obtained. However, different soils have different absorption capacities for various frequency components of leakage signals. The soil with a high elastic modulus can absorb more energy so that the magnitudes of different frequencies of signals are reduced. However, the higher the elastic modulus of the soil, the stronger the energy absorption capacity of the high-frequency part of the signal, which makes the low-frequency component more significant. Therefore, it is more reasonable and accurate for general remote detection to use a sensor with a smaller frequency response but with higher sensitivity to detect the leakage signal.
- The influence of soil with a different elastic modulus on the propagation law of pipeline leakage signal is distinct. For detecting the vibration acceleration signal of water pipeline leakage, it is appropriate that the elastic modulus of the soil covering the pipe of its numerical simulation model is 3.3 times its compressive modulus.
- The pipeline leakage vibration signal has the characteristics of frequency dispersion. The phase velocity of the high-frequency signal is large, while the phase velocity of the low-frequency signal is small. The group velocity of the pipeline leakage vibration signal is affected by the elastic modulus of the surrounding soil. When the elastic modulus of soil is within the range of 7.5–37.5 MPa, the group velocity is about 925 m/s. When the elastic modulus of soil is so large that it has absorbed all high-frequency signals and only low-frequency signals are propagating, the group velocity will decrease significantly.

This study broadens the application of numerical simulation in the transmission characteristics of pipeline leakage vibration signals, helps to understand further the characteristics and transmission characteristics of pipeline leakage vibration signals, and deepens the understanding of the influence of the elastic modulus of soil around the pipeline on the transmission of leakage signals. Furthermore, it provides a basis for the remote detection of leakage signals, improves the accuracy of acoustic emission technology and cross-correlation analysis on leakage detection, and provides the theoretical basis for pipeline leakage detection research.

Author Contributions: Conceptualization, data curation, formal analysis, investigation, methodology, software, validation, visualization, writing—original draft, writing—review and editing, X.Y. (Xuan Yang); funding acquisition, resources, supervision, F.W.; conceptualization, funding acquisition, project administration, resources, supervision, validation, visualization, writing—review and editing,

X.Y. (Xiang Yu); investigation, validation, writing—review and editing, S.L. All authors have read and agreed to the published version of the manuscript.

Funding: This research was funded by the National Key Research and Development Program of China (No. 2022YFC3801000), Key Research & Development and Promotion Projects-Science and Technology in Henan Province (No. 222102320098), the National Natural Science Foundation of China (No. 51978630), and the Program for Guangdong Introducing Innovative and Entrepreneurial Teams (Grant 2016ZT06N340), for which the authors are grateful.

Institutional Review Board Statement: Not applicable.

Informed Consent Statement: Not applicable.

Data Availability Statement: Not applicable.

Acknowledgments: The authors acknowledge the funding support given by the National Key Research and Development Program of China (No. 2022YFC3801000), Key Research & Development and Promotion Projects-Science and Technology in Henan Province (No. 222102320098), the National Natural Science Foundation of China (No. 51978630), and the Program for Guangdong Introducing Innovative and Entrepreneurial Teams (Grant 2016ZT06N340).

Conflicts of Interest: The authors declare no conflict of interest.

References

1. United Nations. *World Population Prospects 2022 Summary of Results*; United Nations: New York, NY, USA, 2022; p. 3.
2. Lu, T.; Liu, Y.; Li, J.; Dong, X. Leakage Situation and Control Solution of China Water Supply Pipeline. *J. Fudan Univ. Nat. Sci.* **2013**, *52*, 807–810+816.
3. Lee, E.J.; Schwab, K.J. Deficiencies in Drinking Water Distribution Systems in Developing Countries. *J. Water Health* **2005**, *3*, 109–127. [CrossRef]
4. Duan, H.F. Development of a TFR-Based Method for the Simultaneous Detection of Leakage and Partial Blockage in Water Supply Pipelines. *J. Hydraul. Eng.* **2020**, *146*, 04020051. [CrossRef]
5. Fontanazza, C.M.; Notaro, V.; Puleo, V.; Nicolosi, P.; Freni, G. Contaminant Intrusion through Leaks in Water Distribution System: Experimental Analysis. *Procedia Eng.* **2015**, *119*, 426–433. [CrossRef]
6. Li, B.; Fang, H.; Yang, K.; Zhang, X.; Du, X.; Wang, N.; Guo, X. Impact of Erosion Voids and Internal Corrosion on Concrete Pipes under Traffic Loads. *Tunn. Undergr. Space Technol.* **2022**, *130*, 104761. [CrossRef]
7. Li, B.; Fang, H.; Zhai, K.; Yang, K.; Zhang, X.; Wang, Y. Mechanical Behavior of Concrete Pipes with Erosion Voids and the Effectiveness Evaluation of the Polyurethane Grouting. *Tunn. Undergr. Space Technol.* **2022**, *129*, 104672. [CrossRef]
8. Liu, J.; Wang, J.; Liu, S.; Qian, X. Feature Extraction and Identification of Leak Acoustic Signal in Water Supply Pipelines Using Correlation Analysis and Lyapunov Exponent. *Vibroengineering Procedia* **2018**, *19*, 182–187. [CrossRef]
9. Ng, K.S.; Chen, P.-Y.; Tseng, Y.-C. A Design of Automatic Water Leak Detection Device. In Proceedings of the 2017 IEEE 2nd International Conference on Opto-Electronic Information Processing (ICOIP), Singapore, 7–9 July 2017; pp. 70–73.
10. Ayala–Cabrera, D.; Herrera, M.; Izquierdo, J.; Ocaña–Levario, S.J.; Pérez–García, R. GPR-Based Water Leak Models in Water Distribution Systems. *Sensors* **2013**, *13*, 15912–15936. [CrossRef]
11. Karkoub, M.; Bouhali, O.; Sheharyar, A. Detection of Leak Acoustic Signal in Buried Gas Pipe. *IEEE Sens. J.* **2021**, *21*, 15544–15553. [CrossRef]
12. Li, J.; Zheng, Q.; Qian, Z.; Yang, X. A Novel Location Algorithm for Pipeline Leakage Based on the Attenuation of Negative Pressure Wave. *Process Saf. Environ.* **2019**, *123*, 309–316. [CrossRef]
13. Wong, L.; Chiu, W.K.; Kodikara, J. Using Distributed Optical Fibre Sensor to Enhance Structural Health Monitoring of a Pipeline Subjected to Hydraulic Transient Excitation. *Struct. Health Monit.* **2018**, *17*, 298–312. [CrossRef]
14. Zuo, J.; Zhang, Y.; Xu, H.; Zhu, X.; Zhao, Z.; Wei, X.; Wang, X. Pipeline Leak Detection Technology Based on Distributed Optical Fiber Acoustic Sensing System. *IEEE Access* **2020**, *8*, 30789–30796. [CrossRef]
15. Ayadi, A.; Ghorbel, O.; BenSalah, M.S.; Abid, M. A Framework of Monitoring Water Pipeline Techniques Based on Sensors Technologies. *J. King Saud Univ.-Comput. Inf. Sci.* **2022**, *34*, 47–57. [CrossRef]
16. Agarwal, N.K. The Sound Field in Fully Developed Turbulent Pipe Flow Due to Internal Flow Separation, Part I: Wall-Pressure Fluctuations. *J. Sound Vib.* **1994**, *169*, 89–109. [CrossRef]
17. Ozevin, D.; Harding, J. Novel Leak Localization in Pressurized Pipeline Networks Using Acoustic Emission and Geometric Connectivity. *Int. J. Press. Vessel. Pip.* **2012**, *92*, 63–69. [CrossRef]
18. Long, R.; Lowe, M.; Cawley, P. Attenuation Characteristics of the Fundamental Modes That Propagate in Buried Iron Water Pipes. *Ultrasonics* **2003**, *41*, 509–519. [CrossRef]
19. Hunaidi, O.; Chu, W.T. Acoustical Characteristics of Leak Signals in Plastic Water Distribution Pipes. *Appl. Acoust.* **1999**, *58*, 235–254. [CrossRef]

20. Long, R.; Vine, K.; Lowe, M.J.S.; Cawley, P. The Effect of Soil Properties on Acoustic Wave Propagation in Buried Iron Water Pipes. *AIP Conf. Proc.* **2002**, *615*, 1310–1317.
21. Yang, J.; Wen, Y.; Li, P. Leak Location Using Blind System Identification in Water Distribution Pipelines. *J. Sound. Vib.* **2008**, *310*, 134–148. [CrossRef]
22. Gao, Y.; Brennan, M.J.; Joseph, P.F. On the Effects of Reflections on Time Delay Estimation for Leak Detection in Buried Plastic Water Pipes. *J. Sound Vib.* **2009**, *325*, 649–663. [CrossRef]
23. Su, D.; Miro, J.V.; Vidal-Calleja, T. Modelling In-Pipe Acoustic Signal Propagation for Condition Assessment of Multi-Layer Water Pipelines. In Proceedings of the 2015 IEEE 10th Conference on Industrial Electronics and Applications (ICIEA), Auckland, New Zealand, 15–17 June 2015; IEEE: Piscataway, NJ, USA, 2015; pp. 545–550.
24. Jing, L.; Li, Z.; Li, Y.; Murch, R.D. Channel Characterization of Acoustic Waveguides Consisting of Straight Gas and Water Pipelines. *IEEE Access* **2018**, *6*, 6807–6819. [CrossRef]
25. Abdullahi, M.; Oyadiji, S.O. Simulation and Experimental Measurement of Acoustic Wave Reflectometry for Leak Detection in Pipes. In Proceedings of the Health Monitoring of Structural and Biological Systems XIII, Denver, CO, USA, 3–7 March 2019; SPIE: Bellingham, WA, USA, 2019; Volume 10972, pp. 376–386.
26. Yan, S.; Yuan, H.; Gao, Y.; Jin, B.; Muggleton, J.M.; Deng, L. On Image Fusion of Ground Surface Vibration for Mapping and Locating Underground Pipeline Leakage: An Experimental Investigation. *Sensors* **2020**, *20*, 1896. [CrossRef] [PubMed]
27. Li, Y.; Zhou, Y.; Fu, M.; Zhou, F.; Chi, Z.; Wang, W. Analysis of Propagation and Distribution Characteristics of Leakage Acoustic Waves in Water Supply Pipelines. *Sensors* **2021**, *21*, 5450. [CrossRef] [PubMed]
28. Wu, J.; Ma, D.; Wang, W. Leakage Identification in Water Distribution Networks Based on XGBoost Algorithm. *J. Water Resour. Plann. Manage.* **2022**, *148*, 04021107. [CrossRef]
29. COMSOL. *COMSOL 5.6: Structural Mechanics Module User's Guide*; COMSOL: Shanghai, China, 2022.
30. Muggleton, J.M.; Brennan, M.J. Leak Noise Propagation and Attenuation in Submerged Plastic Water Pipes. *J. Sound. Vib.* **2004**, *278*, 527–537. [CrossRef]
31. Jia, D.; Shi, F.; Zheng, G.; Xu, S.; An, L. Elastic modulus of soil used in numerical simulation of deep foundation pits. *Chin. J. Geotech. Eng.* **2008**, *30*, 155–158.
32. Bian, A.; Yu, W.; Zhou, H. Progress in the frequency-domain full waveform inversion method. *Prog. Geophys.* **2010**, *25*, 982–993.
33. Carcione, J.M. *Wave Fields in Real Media: Wave Propagation in Anisotropic, Anelastic, Porous and Electromagnetic Media*; Pergamon Press: Trieste, Italy, 2001; ISBN 0-08-043929-2.
34. Liu, Z. Guided Waves in Ultrasonic Nondestructive Testing. *Nondestruct. Test.* **1999**, *21*, 367–369+375.